Journal of the Korean Magnetic Resonance Society **1999**, *3*, 71-83

Nonlinear effects in solution NMR: A numerical study on dynamics of dipolar demagnetizing field and radiation damping

Sangdoo Ahn† and Sanghyuk Lee*

Department of Chemistry, Ewha Womans University, Seoul 120-750, Korea
†Department of Chemistry, Princeton University, Princeton, NJ 08544, USA
Received July 2, 1999

Abstract: The dynamics of the dipolar demagnetizing field is investigated by numerical simulation. The effects of radiation damping, molecular diffusion, and relaxation processes on the dipolar demagnetizing field are examined in terms of the modulation pattern of the z-magnetization and the signal intensity variation. Simulations for multi-components suggest applications for sensitivity enhancement in favorable conditions.

INTRODUCTION

Macroscopic interactions in solution NMR (e.g. dipolar demagnetizing field and radiation damping) have generated significant interest in recent years, in large part because they can produce unexpected peaks in 2D NMR experiments.[1-9] Such effect can become quite dramatic when at least one component is concentrated (for example, in a protonated solvent). Many attempts have been made to remove those effects since they interfere with the conventional cross-peaks in 2D experiments.[10-12]

The theoretical framework which describes these effects has progressed tremendously over the last several years, at least in the limit where one effect dominates. The case which has recently received the most attention is the effects of the dipolar field.[6,13,14] In traditional treatment of magnetic resonance, the magnetic field generated by the bulk magnetization of nuclear spins themselves are neglected. At the high magnetic field strengths currently being used for solution NMR and even in-vivo MRI, however, the bulk magnetization can lead to such unusual phenomena as trains of large amplitude echoes generated by just two RF and quantum theory enables the interpretation of the phenomena as the result of dipolar

couplings between distant spins which can lead to intermolecular multiple quantum coherences (iMQCs).[4,9,15]

Radiation damping also generates unexpectedly complex dynamics. For example, the COSY spectrum of water has many harmonic peaks along the indirectly detected dimension.[1] Analytic solutions by He *et al.*,[3] numerical simulations by Vlassenbroek *et al.*,[7] and numerous later papers showed that radiation damping during the t_2 period is responsible and this was confirmed experimentally by Q-switching.[16] Radiation damping has been an ongoing problem in biological NMR where the solvent peak is usually much larger than others. It creates many artifacts in 2D experiments, and its suppression was intensively investigated.[12] But radiation damping may be constructively used to suppress the water signal in some cases.[17]

This simulation paper shows time evolution of the spatially modulated magnetizations under the dipolar field (DDF) and explores the DDF spin dynamics in the realistic limit where radiation damping, diffusion, and relaxation processes become important. The combination of such processes complicates the evolution of the magnetization tremendously, eliminating any possibility of obtaining analytical solutions. It is worth to note that the quantum picture can still be used to obtain a general understanding of the dynamics. Here we use numerical integration to solve the modified Bloch equations. The effect of each dynamic process will be clearly demonstrated for one and two spin systems in 1D and 2D experiments. Simulations for two-component systems are also performed, which imply possible applications for sensitivity enhancement.

THEORY

Modified Bloch Equations

The time evolution of the uncoupled spins including relaxation processes is described by the Bloch equations:

$$\frac{d\mathbf{M}}{dt} = \gamma \mathbf{M} \times \mathbf{B} - \frac{\left(M_x \hat{\mathbf{x}} + M_y \hat{\mathbf{y}}\right)}{T_2} - \frac{\left(M_z - M_0\right)\hat{\mathbf{z}}}{T_1} \qquad [1]$$

The magnetic field **B** and the magnetization **M** represent local values that may vary as the position of the spins. Interactions with other nuclei in the sample via dipole-dipole interaction and interaction between the magnetization and the receiver coil create additional fields to the applied field. The former is referred to as the dipolar demagnetizing field, and the latter process is radiation damping.

The dipolar demagnetizing field $\mathbf{B_d(r)}$, is a complicated function of position which depends on the spin distribution within the sample. But Deville *et al.* showed that, if the magnetization $\mathbf{M(r)}$ varies only in a single direction s (as can happen if gradient pulses are only applied in a single direction), $\mathbf{B_d(r)}$ could be reduced to a much simpler form:

$$\mathbf{B}_\mathrm{d}(s) = \mu_0 \Delta_s \left[M_z(s)\hat{\mathbf{z}} - \tfrac{1}{3}\mathbf{M}(s) \right] \quad \Delta_s = [3(\hat{\mathbf{s}} \cdot \hat{\mathbf{z}})^2 - 1]/2, \qquad [2]$$

which depends only on the local value of the magnetization.[16] We will assume that the gradient pulses are applied along the z-axis parallel to the main field, giving $\Delta_s = 1$. Warren *et al.* further noted the importance of omitting the average magnetization, yielding a modified equation as[17]

$$\begin{aligned} \mathbf{B}_\mathrm{d}(s) &= \mu_0 \left[\left(M_z(z) - \langle M_z \rangle \right)\hat{\mathbf{z}} - \tfrac{1}{3}\left(\mathbf{M}(z) - \langle \mathbf{M} \rangle \right) \right] \\ &= \mu_0 \left[-\tfrac{1}{3}\left(M_x(z) - \langle M_x \rangle \right)\hat{\mathbf{x}} - \tfrac{1}{3}\left(M_y(z) - \langle M_y \rangle \right)\hat{\mathbf{y}} + \tfrac{2}{3}\left(M_z(z) - \langle M_z \rangle \right)\hat{\mathbf{z}} \right] \end{aligned} \qquad [3]$$

Note that $\langle M_x \rangle$ and $\langle M_y \rangle$ represent the real and imaginary part of the signal that we measure. Therefore the correction terms from the average magnetization play a significant role whenever the signal intensity is not negligible.

The induced current in the coil by the magnetization creates an additional field $\mathbf{B_r}$, which is known as radiation damping.[18] In the presence of inhomogeneous field such as gradient pulses, the original equation for $\mathbf{B_r}$ should be modified to take it into account that it is the average magnetization that induces current in the coil. Then the induced field in the rotating frame can be written as

$$\mathbf{B}_\mathrm{r} = -\frac{\langle M_y \rangle}{\gamma M_0 \tau_r}\hat{\mathbf{x}} + \frac{\langle M_x \rangle}{\gamma M_0 \tau_r}\hat{\mathbf{y}}, \qquad \tau_r = \frac{1}{2\pi\eta M_0 Q\gamma}, \qquad [4]$$

where η is the filling factor and Q is the probe Q-factor. This result agrees with the expressions obtained by Vlassenbroek *et al.*[7] In contrast to the dipolar demagnetizing field, $\mathbf{B_r}$ is independent of position and depends only on the average magnetization. Therefore a pulsed field gradient right after an rf pulse can be used to suppress radiation damping by diminishing the transverse magnetization in an usual situation.

The Bloch equations in the rotating frame that are modified to include the dipolar demagnetizing field, radiation damping, diffusion and relaxation processes can be written as

$$\begin{aligned}
\frac{\delta M_x}{\delta t} &= \Delta\omega M_y + \frac{M_y M_z}{M_0\tau_d} - \frac{2M_y\langle M_z\rangle}{3M_0\tau_d} - \frac{\langle M_y\rangle M_z}{3M_0\tau_d} - \frac{\langle M_x\rangle M_z}{M_0\tau_r} + D\frac{d^2M_x}{dz^2} - \frac{M_x}{T_2} \\
\frac{\delta M_y}{\delta t} &= -\Delta\omega M_x - \frac{M_x M_z}{M_0\tau_d} + \frac{2M_x\langle M_z\rangle}{3M_0\tau_d} + \frac{\langle M_x\rangle M_z}{3M_0\tau_d} - \frac{\langle M_y\rangle M_z}{M_0\tau_r} + D\frac{d^2M_y}{dz^2} - \frac{M_y}{T_2} \\
\frac{\delta M_z}{\delta t} &= \frac{M_x\langle M_y\rangle - \langle M_x\rangle M_y}{3M_0\tau_d} + \frac{M_x\langle M_x\rangle + M_y\langle M_y\rangle}{M_0\tau_r} + D\frac{d^2M_z}{dz^2} - \frac{M_z - M_0}{T_1}
\end{aligned} \quad [5]$$

where $\tau_d = (\gamma\mu_0 M_0)^{-1}$ is the characteristic dipolar demagnetizing time. For pure water sample in our Varian 600 MHz NMR spectrometer, the two characteristic time constants are $\tau_d \approx 67$ ms, $\tau_r \approx 12$ ms. Therefore radiation damping usually dominates the short time behavior if average transverse magnetization is significant. A gradient pulse may be used to purge the magnetization, and radiation damping will be suppressed. Since both characteristic time constants are inversely proportional to the gyromagnetic ratio and spin concentration, these effect becomes important when we have concentrated proton spins in the sample. Eq. [5] fully defines the time evolution of a single spin as is the case for samples containing solvent only.

A mixture of two types of noninteracting spins 1/2 would be more relevant to the real experiments. Extending Eq. [5] for two component system requires simply adding contribution from the second spin when the induced field is calculated in Eqs. [3] and [4]. Additional terms in the derivative expression are:

$$\begin{aligned}
\frac{\delta M_{x1}}{\delta t} &= \begin{pmatrix}\text{terms in}\\ \text{Eq.[5]}\end{pmatrix} + \frac{2M_{y1}M_{z2}}{3M_{01}\tau_{d1}} + \frac{M_{y2}M_{z1}}{3M_{01}\tau_{d1}} - \frac{2M_{y1}\langle M_{z2}\rangle}{3M_{01}\tau_{d1}} - \frac{\langle M_{y2}\rangle M_{z1}}{3M_{01}\tau_{d1}} - \frac{\gamma_1\langle M_{x2}\rangle M_{z1}}{\gamma_2 M_{02}\tau_{r2}} \\
\frac{\delta M_{y1}}{\delta t} &= \cdots - \frac{2M_{x1}M_{z2}}{3M_{01}\tau_{d1}} - \frac{M_{x2}M_{z1}}{3M_{01}\tau_{d1}} + \frac{2M_{x1}\langle M_{z2}\rangle}{3M_{01}\tau_{d1}} + \frac{\langle M_{x2}\rangle M_{z1}}{3M_{01}\tau_{d1}} - \frac{\gamma_1\langle M_{y2}\rangle M_{z1}}{\gamma_2 M_{02}\tau_{r2}} \\
\frac{\delta M_{z1}}{\delta t} &= \cdots - \frac{M_{x1}M_{y2} - M_{x2}M_{y1}}{3M_{01}\tau_{d1}} + \frac{M_{x1}\langle M_{y2}\rangle - \langle M_{x2}\rangle M_{y1}}{3M_{01}\tau_{d1}} + \frac{M_{x1}\langle M_{x2}\rangle + M_{y1}\langle M_{y2}\rangle}{\gamma_2 M_{02}\tau_{r2}/\gamma_1}
\end{aligned} \quad [6]$$

The Bloch equations for spin 2 can be obtained by swapping indices 1 and 2 in Eq. [6].

If the two spins are hetero-nuclei, the rotating frames for spin 1 and 2 have vastly different angular frequencies. Transverse terms of the other spin can be ignored in Eq. [6] since its effect will be averaged out in time $t >> 1/(\gamma_1 - \gamma_2)B_0 \approx 0.1\mu s$. Then Eq. [6] can be further simplified to

$$\frac{\delta M_{x1}}{\delta t} = \begin{pmatrix} \text{terms in} \\ \text{Eq.[5]} \end{pmatrix} + \frac{2M_{y1}M_{z2}}{3M_{01}\tau_{d1}} - \frac{2M_{y1}\langle M_{z2}\rangle}{3M_{01}\tau_{d1}}$$

$$\frac{\delta M_{y1}}{\delta t} = \begin{pmatrix} \text{terms in} \\ \text{Eq.[5]} \end{pmatrix} - \frac{2M_{x1}M_{z2}}{3M_{01}\tau_{d1}} + \frac{2M_{x1}\langle M_{z2}\rangle}{3M_{01}\tau_{d1}}, \quad \frac{\delta M_{z1}}{\delta t} = \begin{pmatrix} \text{terms in} \\ \text{Eq.[5]} \end{pmatrix} \qquad [7]$$

Numerical Simulation

The Bloch equations were numerically integrated by using the fifth-order Cash-Karp Runge-Kutta method, which monitors local truncation error to ensure accuracy and to control adaptive stepsize.[19] The gradient pulses were assumed to be applied along the z-direction. The active volume within the sample were divided into many horizontal slices to deal with pulsed gradients and translational diffusion. We need separate Bloch equations for each slice since i) the magnetic field is different for each slice in the presence of gradient pulses, ii) the initial conditions for magnetization vectors in each slice are difference in the subsequent evolution periods, iii) the dipolar demagnetizing field are different from slices to slices.

The second derivative for diffusion may be calculated in fully explicit way as[19]

$$\frac{\delta \mathbf{M}(j)}{\delta t} = D\frac{\mathbf{M}(j+1) - 2\mathbf{M}(j) + \mathbf{M}(j-1)}{(\Delta z)^2}, \qquad [8]$$

where $\mathbf{M}(j)$ indicates the magnetization of the current slice and $\mathbf{M}(j \pm 1)$ are those in the adjacent slices. Δz defines the thickness of the slice. A molecule can diffuse out of the active region or the reverse can happen in a real experiment. To alleviate this edge boundary effect, a decaying Gaussian-type weighting function was multiplied for slices close to the top and bottom edges.

The simulation will be mostly confined to CRAZED-related experiments even though the program was written to support any arbitrary pulse sequences for one or two spin system (e.g., 1D/2D, homonuclear or heteronuclear experiments with selective pulses). All simulations used 3,000 slices to cover approximately 1 cm active region in the sample. $\mathbf{M}_1$ and $\mathbf{M}_2$ in each slice have six components. Magnetizations in different slices are coupled via diffusion. The six components within each slice are coupled via dipolar demagnetizing field and/or radiation damping. The average magnetization coupled the whole slices anyway. Therefore we have 18,000 coupled differential equations to solve. Each 1D simulation took about 2 minutes and 2D simulation took about 2-4 hours in Silicon Graphic Indigo 2 workstation. The signal was calculated by averaging the transverse magnetizations in all slices.

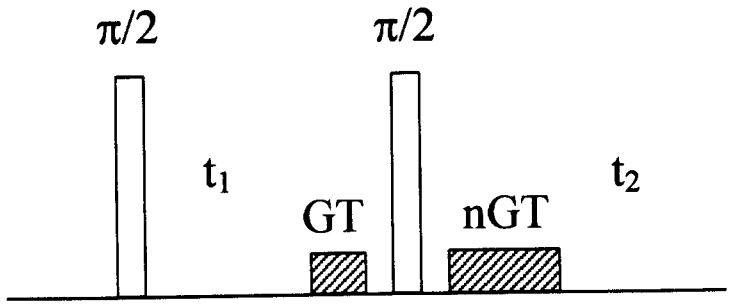

Fig. 1. The nQ-CRAZED pulse sequence. The gradient strength of 10 gauss was used throughout the simulation. The duration of the first gradient pulse was 1 ms.

RESULTS AND DISCUSSION

We simulate spectra from the CRAZED pulse sequence shown in Fig. 1, which served as a prototype experiment to show the effect of dipolar demagnetizing field.[4] The first gradient pulse creates a magnetization helix along the z-direction. The second rf pulse transforms the magnetization helix into the modulated z-magnetization, i.e. $M_z(z) \propto \cos(\gamma GTz)$, which the dipolar demagnetizing field is proportional to (cf. Eq. [2]). Therefore the local magnetic field becomes sinusoidally modulated along the gradient direction during the t_2 period as shown "DDF only" in Fig. 2. This nonlinear effect creates many unexpected results such as multiple spin echoes or nQ-CRAZED peaks.

In this section, we are going to simulate FID's in t_2 period with various dynamic processes in. An analytical solution can be calculated if only dipolar demagnetizing field is considered as in Eq. [2] without the effect of average magnetizations, ignoring all other dynamics such as relaxation, diffusion, and radiation damping. The signal from nQ-CRAZED experiment for one component system is shown to be[15]

$$M^+(t_1,t_2) = i^{n-1} M_0 e^{-in\Delta\omega t_1} e^{i\Delta\omega t_2} n\left(\frac{\tau_d}{t_2}\right) J_n\left(-\frac{t_2}{\tau_d}\right), \qquad [9]$$

where J_n is the n-th order Bessel function. FID's from 2Q-CRAZED experiments with (corrected) and without (uncorrected) the effect of average magnetizations are shown in

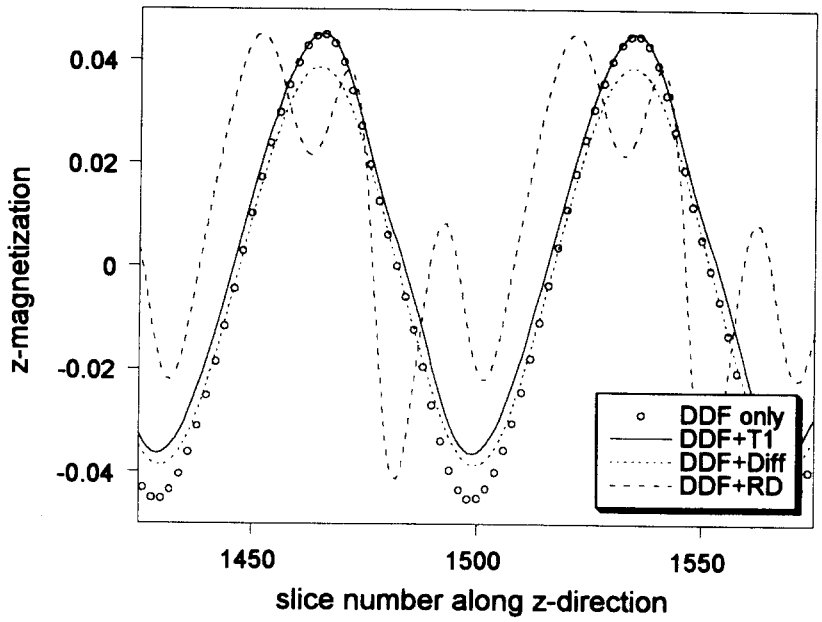

Fig. 2. Modulation patterns of the z-magnetization across slices near the center at t_2=100 ms. Each line shows the z-magnetization across the slices when the corresponding dynamics are active in the pulse sequence. The dipolar demagnetizing field (DDF) corrected for the effect of average magnetization was used. τ_d = 67 ms, τ_r = 12 ms, D=1.85×10^{-5} cm^2 sec^{-1}.

Fig. 3. $\Delta\omega$ was set to zero for convenience in representation. The maximum intensity of the signal becomes larger with average magnetizations in. A numerical experiment shows that this is mainly due to the transverse components of average magnetization — i.e. $\langle M_x \rangle$ and $\langle M_y \rangle$ in Eq. [3]. The longitudinal average magnetization causes little change. All the simulations following includes the effect of average magnetizations whenever the dipolar demagnetizing field (DDF) is used.

Spin relaxation processes greatly influence the signal from the dipolar demagnetizing field, which is shown in Fig. 3 for 2Q-CRAZED case. While both processes reducing the intensity, T_1 process changes the signal pattern completely, whereas T_2 simply scales down the signal. This can be explained by considering the effect of T_1 relaxation during the t_2 period. M_z pointing toward –z direction experiences greater change due to the T_1 relaxation process, reducing the modulation amplitude and distorting modulation shape

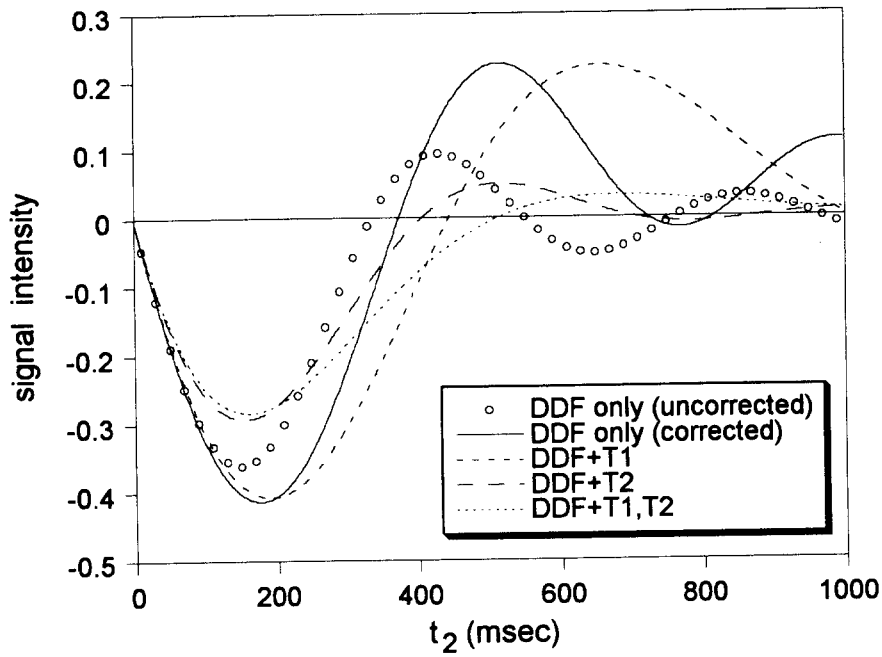

Fig. 3. Effect of average magnetization and relaxation processes. FID's from water proton in 2Q-CRAZED experiment are plotted. t_1 = 10 ms was used. Relaxation constants of T_1 = 1 sec, T_2 = 0.5 sec were used in the corresponding simulations.

of the z-magnetization (see Fig. 2). This causes the signal deviate from the expected Bessel function. T_2 relaxation just reduces the transverse components, and does not perturb the dipolar demagnetizing field substantially. Therefore the signal does not change much from its original shape.

Molecular diffusion also makes the magnetization helix fade away as the T_1 relaxation, thereby reducing the signal. But it causes the magnetization decay to zero rather than to the equilibrium value as would be the case for T_1 relaxation (cf. Fig. 2). The other difference is that the diffusional effect is identical for M_x, M_y, and M_z. Fig. 4 shows the effect of molecular diffusion in the presence of relaxation processes for 2Q- and 4Q-CRAZED signals. Diffusion has greater influence on the positive 4Q-CRAZED signal. This can be readily explained when we consider the quantum mechanical source of the signal, i.e. *inter*molecular multiple quantum coherence (iMQC).[4,15] It is quite natural that the four-spin intermolecular multiple quantum coherence be affected more readily by the diffusion than the two-spin coherence. Another reason is that diffusion has more time to reduce the

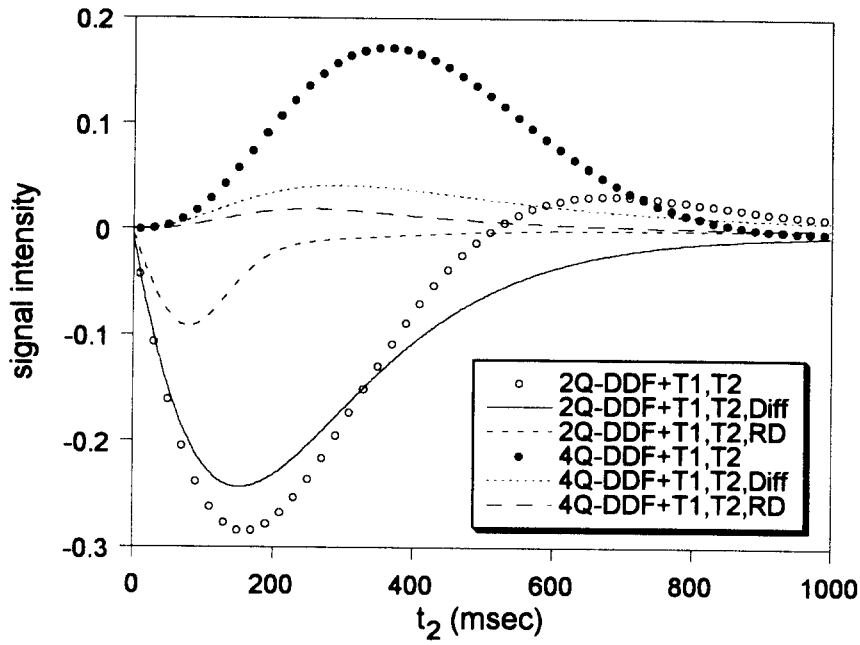

Fig. 4. Effect of molecular diffusion and radiation damping on 2Q-(negative) and 4Q-(positive) CRAZED signals. Parameters used for simulation are the same as Figs. 2 and 3.

signal in 4Q case since the maximum intensity of 4Q signal appears later than 2Q signal.

Radiation damping reduces the CRAZED signal significantly as can be seen in Fig. 4. The dynamics due to radiation damping may be written as $d\theta/dt = -\sin\theta/\tau_r$, where θ is the angle between the magnetization vector and the magnetic field.[18] It reduces the angle without changing length of the magnetization vector when the transverse magnetization is not negligible. During the t_1 period, radiation damping converts part of the transverse magnetization to the longitudinal one. Therefore the "effective" flip angle of the first pulse becomes less than 90°, and the signal becomes weaker. A strong gradient pulse following the rf pulse destroys the transverse magnetization, and radiation damping may be ignored during the subsequent delay. Therefore placing part of the first gradient pulse right after the first rf pulse recovers the reduced intensity due to radiation damping during the t_1 period completely. It was verified by numerical simulation (not actually shown).

Radiation damping during the t_2 period is somewhat more tricky. Even though we have the second gradient, its role is not destroying the transverse magnetization, but refocusing nQ-signal in CRAZED sequence. Radiation damping can not be ignored during the t_2 period since the signal grows initially in the detection period. Radiation damping

rotates this growing magnetization toward the z-axis, thus reducing the signal intensity too. Increased z-magnetization does not change the dipolar demagnetizing field significantly since it is unmodulated one. In this sense, the role of radiation damping might be thought to be rather similar to T_2 relaxation process since the transverse magnetization is reduced and the increased longitudinal magnetization does not alter the dipolar demagnetizing field much.

Detailed dynamics of radiation damping is much more complicated due to its nonlinearity in the Bloch equations. For example, COSY spectrum of water has many harmonic peaks along the indirectly detected dimension.[1] Vlassenbroek *et al.* showed from their numerical simulation study that radiation damping during the t_2 period is responsible,[7] and this was confirmed experimentally by Q-switching method.[20] Their view of radiation damping as a "soft" pulse readily explains multiple spin echoes or harmonics in water, even though its role is not as clear in CRAZED sequence. The z-magnetization after evolving 100 ms under radiation damping and the dipolar demagnetizing field obtains an additional modulation frequency as can be seen in Fig. 2. This nonlinearity can cause a lot of unexpected results in 2D experiments.

The signal from the CRAZED experiment for two component systems (homo- and/or hetero-nuclear spins), ignoring all other dynamics, can be written as[21]

$$M_1^+ = i^{n-1+k\left(1-\frac{\gamma_2}{\gamma_1}\right)} M_{10} \exp\left\{-i\left(n-k\frac{\gamma_2}{\gamma_1}\right)\Delta\omega_1 t_1\right\} \exp(-ik\Delta\omega_2 t_1) \exp(i\Delta\omega_1 t_2) \times \left(n-k\frac{\gamma_2}{\gamma_1}\right)\left(\frac{\tau_{d1}}{t_2}\right) J_{n-k\frac{\gamma_2}{\gamma_1}}\left(-\frac{t_2}{\tau_{d1}}\right) J_k\left(-\frac{2}{3}\frac{\gamma_1}{\gamma_2}\frac{t_2}{\tau_{d2}}\right) \quad [10]$$

We simulate spectra for mixture of two spins with nonlinear dynamics based on Eq. [7]. Fig. 5 shows simulation (when we detect proton magnetization) for the double-quantum coherence in a representative hetero-nuclear system, ^{1}H and ^{13}C, with a 100:1 concentration ratio between two nuclei (corresponding to a 1600:1 magnetization ratio). To select ^{1}H-^{13}C double quantum coherences, the ratio between two gradient pulses used in this simulation has been set 1:1.25 (see the inset in Fig. 5). Simulations without the demagnetizing field give no signal whether radiation damping is included or not. Other dynamics reduce the signal intensity significantly. These kind of experiments have strongly suggested applications towards indirect detection of low-γ nuclei by observing high-γ nuclei.[22,23]

Fig. 6 shows 2D simulation for homonuclear two components whose T_2 relaxation times are significantly different (500 and 5 msec). Only 2Q-coherences from different spins were selected by a simple phase cycling. The signal from these intermolecular coherences

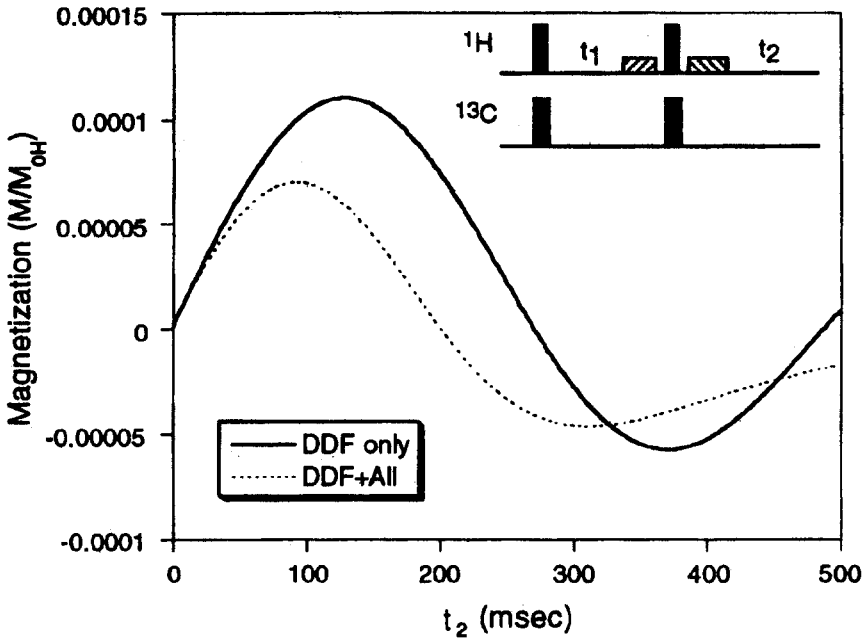

Fig. 5. A simulation for ^{1}H-^{13}C 2Q-coherence (in a 100:1 concentration ratio). FID's from proton are plotted. The dynamic parameters for proton are the same as in Fig. 2. The relaxation times of T_1 = 5 sec, T_2 = 3 sec were used for carbon. A gradient ratio of 1:1.25 selects only heteronuclear double-quantum terms.

persists for relatively long period even though one of the spins has very short relaxation time (compare with the fastly decaying FID of the spin in the same pulse sequence without gradient pulses). This result implies that the information on fastly decaying magnetizations may be obtained by detecting the intermolecular multiple quantum coherences coupled with spins of longer relaxation time.

Acknowledgment

This work was supported by the nondirected research fund of the Korea Research Foundation. S. Lee is grateful to W. S. Warren for invitation to Princeton University during the summer of 1998.

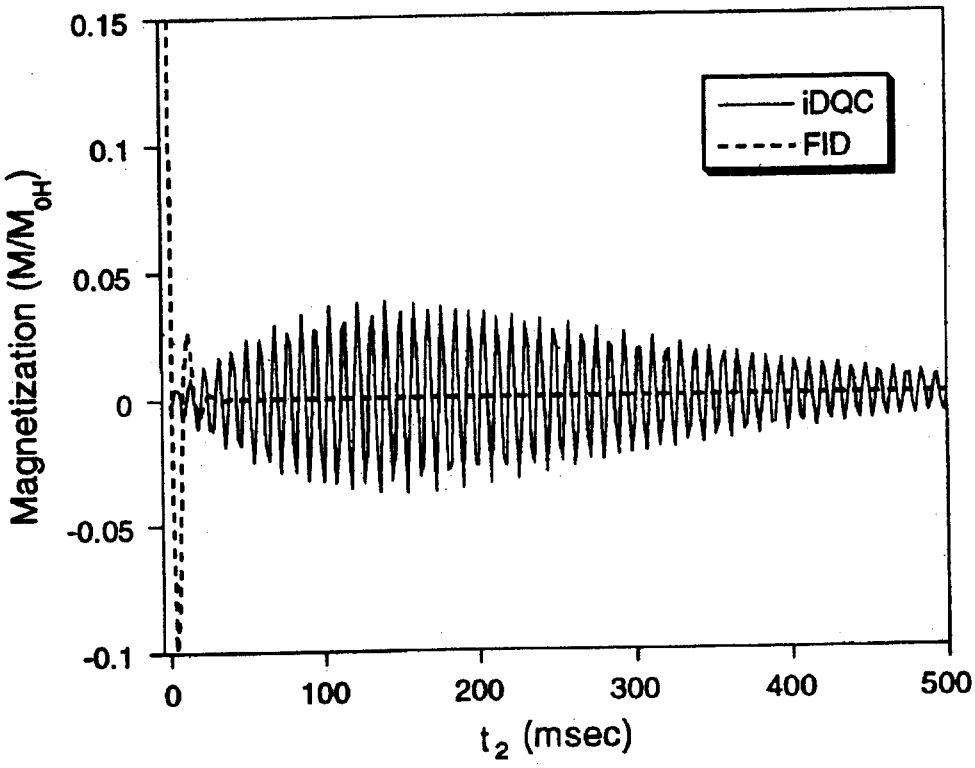

Fig. 6. A simulation for homonuclear two spin 2Q-coherence that have different relaxation times, T_{2s} = 0.5 sec, T_{2f} = 0.005 sec, and T_{1s} = T_{2f} = 1 sec. The proton concentration of 30 M and the radiation damping time of 40 ms were used for both spins. Only 2Q-coherences from different spins were selected by a simple phase cycling. The dotted line is the FID of the spin having short T_2 (0.005 sec) without gradient pulses.

RERERENCES

1. M. McCoy and W. S. Warren, *J. Chem. Phys.* **93**, 858(1990).
2. R. Bowtell, R. M. Bowley, and P. Glover, *J. Magn. Reson.* **88**, 643(1990).
3. Q. He, W. Richter, S. Vathyam, and W. S. Warren, *J. Chem. Phys.* **98**, 6779(1993).
4. W. S. Warren, W. Richter, A. H. Andreotti, and S. Farmer, *Science* **262**, 2005(1993).
5. S. Ahn and W. S. Warren, *Chem. Phys. Lett.* **291**, 121(1998).
6. W. Richter, S. Lee, W. S. Warren, and Q. He, *Science* **267**, 654(1995).

7. A. Vlassenbroek, J. Jeener, and P. Broekaert, *J. Chem. Phys.* **103**, 5886(1995).
8. J. Jeener, A. Vlassenbroek, and P. Broekaert, *J. Chem. Phys.* **103**, 1309 (1995).
9. S. Ahn, W. S. Warren , and S. Lee, *Mol. Phys.* **95**, 769(1999).
10. V. Sklenar, *J. Magn. Reson. A* **114**, 132(1994).
11. P. C. M. van Zijl, M. O. Johnson, R. H. Hurd, *J. Magn. Reson. A* **113**, 265(1995).
12. H. Barjat, D. L. Mattiollo, and R. Freeman, *J. Magn. Reson.* **136**, 114(1999).
13. R. Bowtell and P. Robyr, *Phys. Rev. Lett.* **76**, 4971(1996).
14. W. S. Warren, S. Ahn, R. R. Rizi, J. Hopkins, J. S. Leigh, M. Mescher, W. Richter, M. Gardwood, and K. Ugurbil, *Science* **281**, 247(1998).
15. S. Lee, W. Richter, S. Vathyam, and W. S. Warren, *J. Chem. Phys.* **105**, 874(1996).
16. G. Deville, M. Bernier, and J. M. Derieux, *Phys. Rev. B* **19**, 5666 (1979).
17. W. S. Warren, S. Lee, W. Richter, and S. Vathyam, *Chem. Phys. Lett.* **247**, 207(1995).
18. N. Bloembergen, E. M. purcell, and R. V. Pound, *Phys. Rev.* **73**, 679(1948).
19. W. H. Press, S. A. Teukolsky, W. T. Vetterling, and B. P. Flannery, Numerical Recipes 2nd ed., Press, NewYork (1992).
20. C. E. Ball, G. J. Bowden, T. H. Haseltine, M. J. Prandolini, and W. Bermer, *Chem. Phys. Lett.* **261**, 421(1996).
21. S. Ahn, W. S. Warren, and S. Lee, *J. Magn. Reson.* **128**, 114(1997).
22. R. Bowtell, *J. Magn. Reson.* **100**, 1(1992).
23. W. S. Warren, and S. Ahn, *J. Chem. Phys.* **108**, 1013(1998).